Arch. Metall. Mater. **66** (2021), 1, 171-180

DOI: 10.24425/amm.2021.134773

BINGXIN WANG[1*], YINGTIAN JIANG[1]

FORMATION AND THERMODYNAMIC ANALYSES OF INCLUSIONS IN Ti-CONTAINING STEEL WELD METALS WITH DIFFERENT Al CONTENTS

Ti-containing steel weld metals with Al contents of 0.01-0.085% were prepared. The effects of Al contents on the inclusions evolution were investigated by means of thermodynamic calculations coupled with electron probe micro-analyses and transmission electron microscopy. The results show that the inclusions in the 0.01% Al weld metal are mainly composed of ilmenite with some amounts of (Mn-Si-Al)-oxide and titanial_spinel. When Al content is increased up to 0.035%, a more amount of corundum and a small amount of pseudobrookite are formed. In 0.085% Al weld metal, the (Mn-Si-Al)-oxide disappears completely, and the inclusions contain a substantial amount of corundum, in addition to a minimal amount of pseudobrookite. Ti_3O_5, $MnTi_2O_4$ and $MnTiO_3$ are the primary constituents of pseudobrookite, titanial_spinel and ilmenite, respectively. Titanial_spinel and ilmenite have higher amounts of Mn, but lower Ti levels compared with pseudobrookite. In the case of presence of a considerable amounts of titanial_spinel and ilmenite, Mn-depleted zone is formed in matrix around the inclusions.

Keywords: Thermodynamic calculation, Electron probe micro-analyzer, Oxide inclusion, Aluminium content, Phase diagram

1. Introduction

It is well known that Ti-containing oxide inclusions such as TiO [1], Ti_2O_3 [2], $MnTi_2O_4$ [3] and $MnTiO_3$ [4] in weld metals and/or steels can strongly contribute to the nucleation of acicular ferrite, which can noticeably improve the toughness. Thus, accurate control of the formation of such inclusions is very important. The chemical compositions of steels and/or weld metals have strong effect on the formation of inclusions. Researchers investigated the influences of Ti [5], Zr [6], Mg [7,8] elements, etc., on the inclusions formation. As a strong deoxidizer, Al is usually used to deoxidize the liquid Fe solution. Therefore, the steels and/or weld metals inevitably contain a certain amount of Al. However, so far few studies have been done to investigate the effect of Al element on the evolution of the inclusions in Ti-containing weld metals.

On the other hand, the formation of inclusions is rather complex because the inclusions usually consist of a mixture of several complex crystalline solid solutions and/or amorphous phases instead of simple stoichiometric compounds mentioned above [9]. Therefore, it is a little difficult to accurately analyze the types, contents and of chemical compositions of constituent phases in inclusions only by means of experimental ways. By FactSageTM, thermodynamic calculation approach can be used to effectively predict the formation of multi-phase inclusions [10-12].

The present study analyzed how Al element affects the inclusions evolution including the types, contents and of chemical compositions of constituent phases of inclusions in Ti-containing steel weld metals using FactSage thermochemical computing package combined with electron probe micro-analyzer and transmission electron microscope.

2. Experimental procedure

2.1. Weld metals preparation

Figure 1 indicates the process of weld metals preparation. Build-up welding using pure Fe powder was first performed in a 15 mm deep trapezoid slot in C-Mn steel plates, and then a V-groove with depth of 7 mm is again machined at the build-up welds. After that, a single pass submerged-arc welding (SAW) process is performed using a C-Mn steel welding wire. Three weld metals with different Al contents, but almost the same Ti and Mn concentrations were obtained by adding different amounts of pure Al powder and a certain amounts of Ti-Fe powder (33% Ti)

[1] LIAONING SHIHUA UNIVERSITY, COLLEGE OF MECHANICAL ENGINEERING, FUSHUN 113001, CHINA

* Corresponding author: wangbingxin@163.com

and Mn-Fe powder (81% Mn) to the groove prior to SAW. The chemical compositions of the welding wire and weld metals are listed in Tables 1 and 2, respectively. In light of the Al content, weld metals were labeled as WL (0. 01% Al), WM (0.035% Al) and WH (0.085% Al).

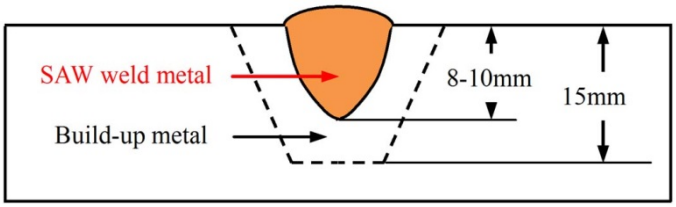

Fig. 1. The schematic drawing showing the preparation of the weld metal

TABLE 1

Chemical compositions of welding wire (mass, %)

C	Mn	Si	S	P	Al
0.05	0.86	0.06	0.022	0.02	0.01

TABLE 2

Chemical compositions of weld metals (mass, %)

C	Mn	Si	S	P	Al	O	N	Ti
0.050	3.01	0.203	0.014	0.029	0.010	0.040	0.0037	0.018
0.045	3.14	0.220	0.016	0.025	0.035	0.039	0.0041	0.020
0.056	2.98	0.271	0.014	0.026	0.085	0.037	0.0039	0.018

2.2. Inclusion analyses and thermochemical computing on the formation of inclusion

The specimens were cut from the weld metals, and examination planes perpendicular to the welding direction were prepared by mechanical polishing. The chemical compositions of the inclusions were analyzed by a JEOL JXA-8530F electron probe micro-analyzer (EPMA).

Transmission electron microscopy (TEM) analysis was conducted to investigate the crystal structure and the phase identification for the inclusions using selected area electron diffraction patterns (SADP).

The slices with 0.3 mm thickness machined along the examination planes were mechanically thinned to 80 μm, followed by twin-jet electropolishing in an electrolyte of 8% perchloric acid and 92% ethanol at the temperature of –30°C. After that, the thin foil specimens for TEM were obtained by several ion milling steps, and were examined using an FEI Tecnai G2 F20 at an operating voltage of 200 kV.

FactSageTM (version 7.2) was employed to calculate the thermodynamic stability of various inclusion phases using the FToxid, FTmisc and FSstel databases. The major constituent phases of inclusion considered in the present thermochemical calculations are as followed:

- Pseudobrookite: Ti_3O_5-$FeTi_2O_5$-$MnTi_2O_5$ solid solution,
- Titanial_Spinel: $(Mn, Fe)(Ti, Al)_2O_4$ solid solution,
- Ilmenite: Ti_2O_3-$FeTiO_3$-$MnTiO_3$ solid solution,
- Corundum: Al_2O_3+(Ti_2O_3 in dilute amount),
- Stoichiometric compounds: all relevant stoichiometric compounds, namely $Mn_2Al_4Si_5O_{18}$ and MnS,
- Slag phase: Al_2O_3-SiO_2-MnO-Ti_2O_3-TiO_2-FeO multi-component liquid oxides solution.

Equilibrium calculations were performed between 1000-1600°C to predict the formation of inclusions. Moreover, during further cooling in the solid state, various reactions including the precipitations of oxides and nitrides from matrix due to the decrease in solubility, were not considered, for simplicity.

3. Results and discussion

Figures 2-4 present the EPMA analysis results of inclusions in the weld metals containing different levels of Al. According to the chemical composition characteristics displayed in EPMA maps of the inclusions, the inclusion in WL is mainly composed of the (Mn-Si-Al)-oxide and (Mn-Ti)-oxide accompanied by a certain amount of Al-containing oxide phase and small amount of discrete MnS patches distributed at the periphery of the inclusion. Compared with the inclusion in WL, the amounts of (Mn-Ti)-oxide and Al-containing oxide of the inclusion in WM are increased, and (Mn-Si-Al)-oxide nearly disappears. In WH, as shown from EPMA maps, the Mn and Si element contents in the inclusion are lower than those of the matrix located near the inclusion. Due to the absence of Mn and Si, the inclusion predominantly consists of Al-oxide, and does not contain (Mn-Si-Al)-oxide. Moreover, the inclusion also has minimal amount of Ti-rich constituent. During the steel cooling, in addition to Ti-oxide, Ti-nitride inclusion can also be precipitated from the steel matrix because of the decrease in the solubilities of Ti and N. Therefore, EPMA analyses including N element of another inclusion in WH were conducted again to identify the Ti-rich constituent from the point of view of chemical compositions, and the analysis results are shown in Figure 5. Obviously, the inclusion does not contain N element, indicating that Ti-rich area in the inclusion in WH should be Ti-containing oxide phase rather thanTi-nitride.

Figure 6 presents the thermodynamic analyses about inclusions evolution. It can be clearly observed from the constituent phases of the inclusions at 1000°C (liquid oxides have been completely decomposed at this temperature) that, in WL, the inclusion contains a large amount of ilmenite solid solution in addition to more amounts of $Mn_2Al_4Si_5O_{18}$ and titanial_spinel. In WM, a large amount of corundum and a small amount of pseudobrookite are formed. Moreover, titanial_spinel solid solution and $Mn_2Al_4Si_5O_{18}$ compound disappear. In WH, the inclusion is mainly composed of corundum with minimal amount of pseudobrookite.

The constituent contents and chemical compositions of solid solution in the inclusions were obtained based on the thermodynamic calculation results, and shown in Tables 3 and 4, respectively. $MnTi_2O_4$, $MnTiO_3$, Ti_3O_5 and Al_2O_3 are the primary

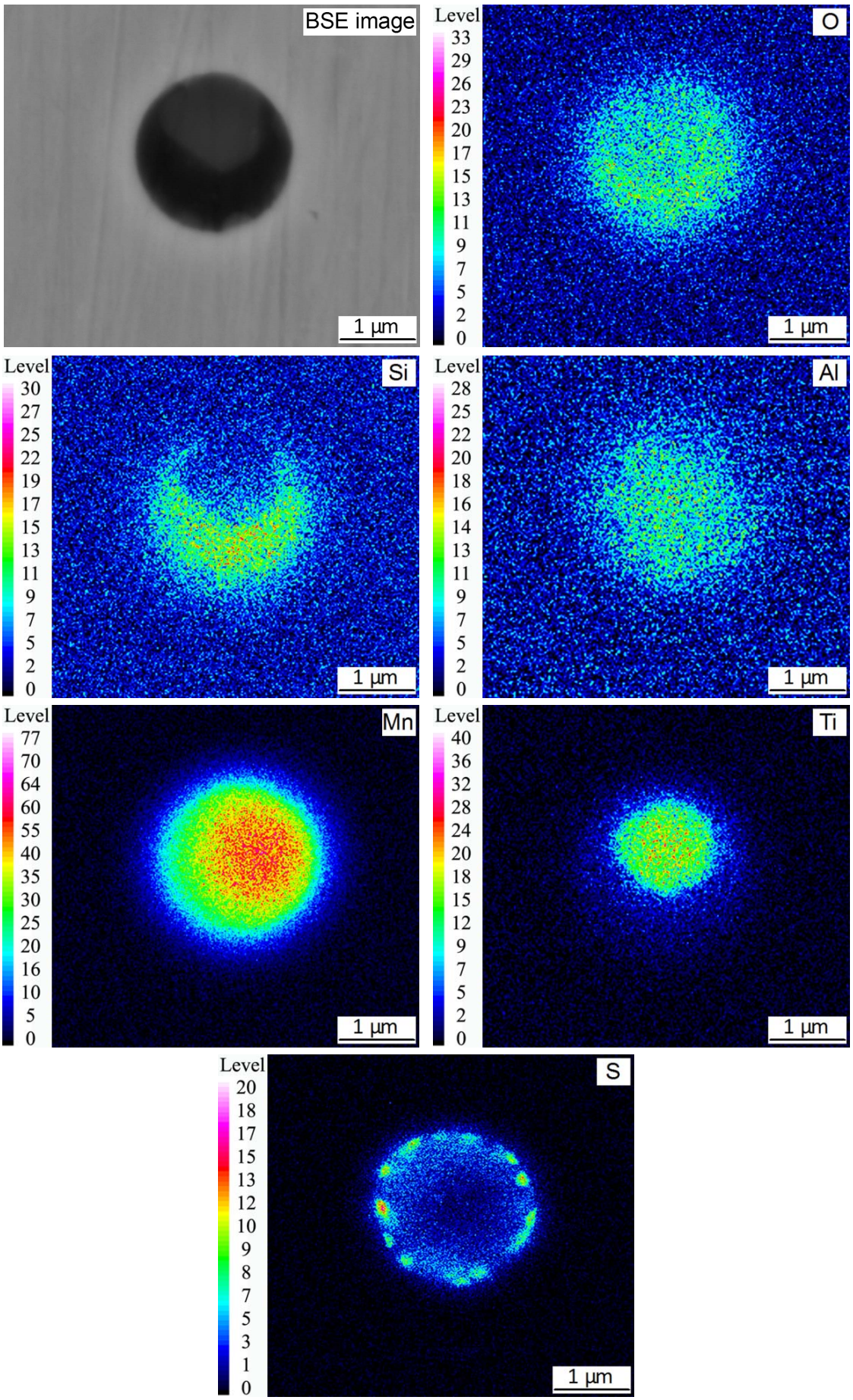

Fig. 2. Backscattered electron (BSE) image and EPMA maps of the inclusion in WL showing the morphology and element characteristics of inclusion

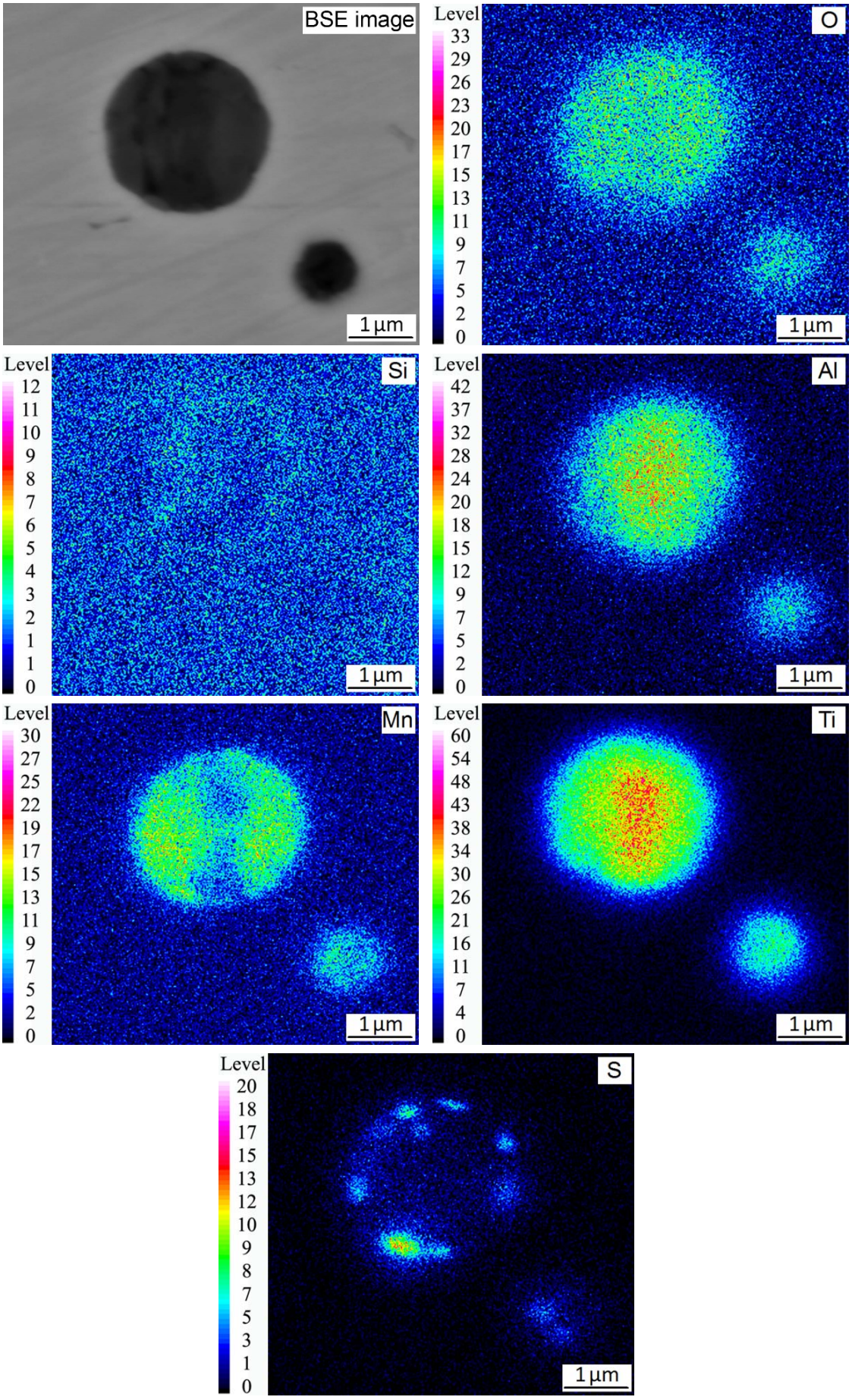

Fig. 3. Backscattered electron (BSE) image and EPMA maps of the inclusion in WM showing the morphology and element characteristics of inclusion

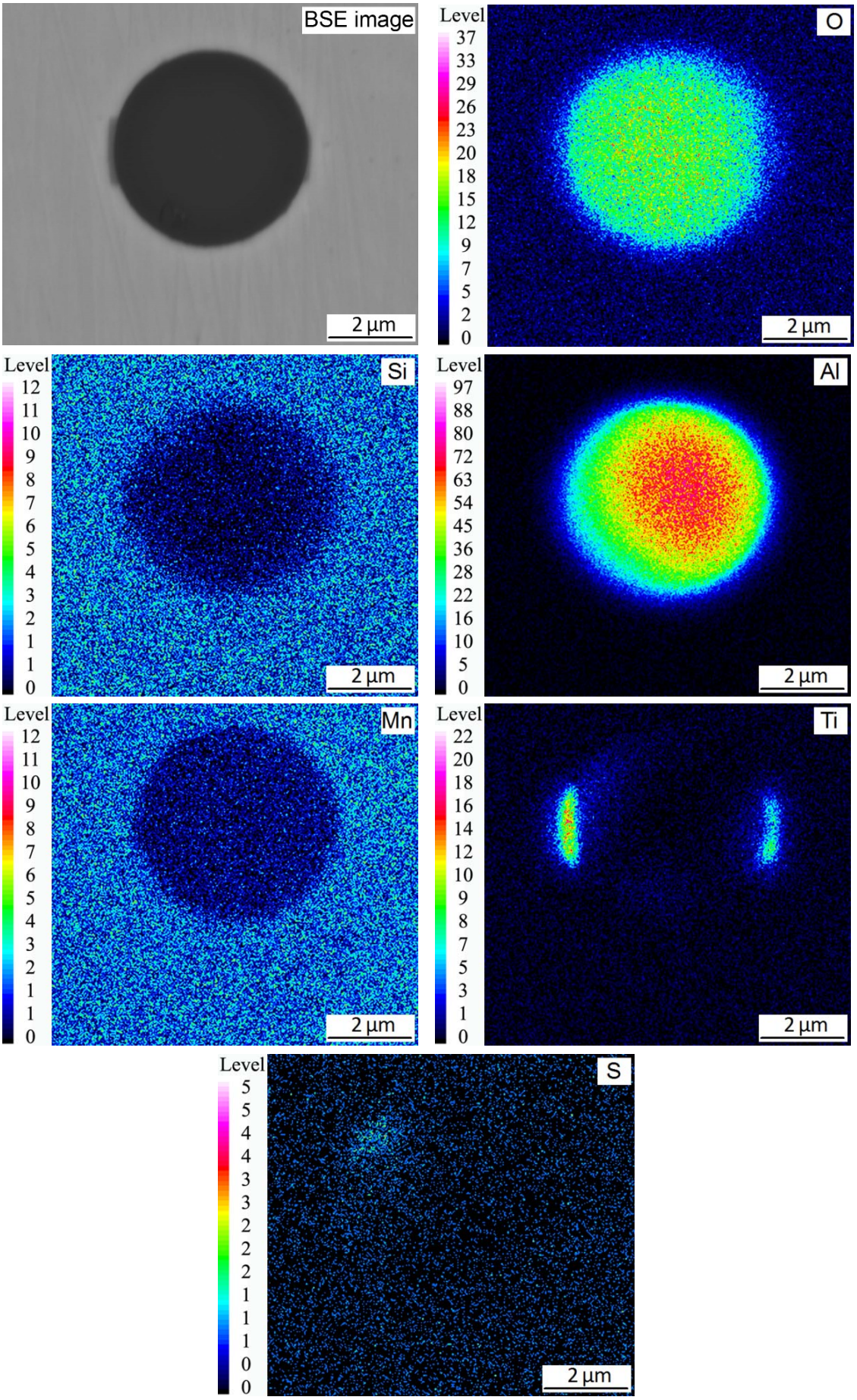

Fig. 4. Backscattered electron (BSE) image and EPMA maps of the inclusion in WH showing the morphology and element characteristics of inclusion

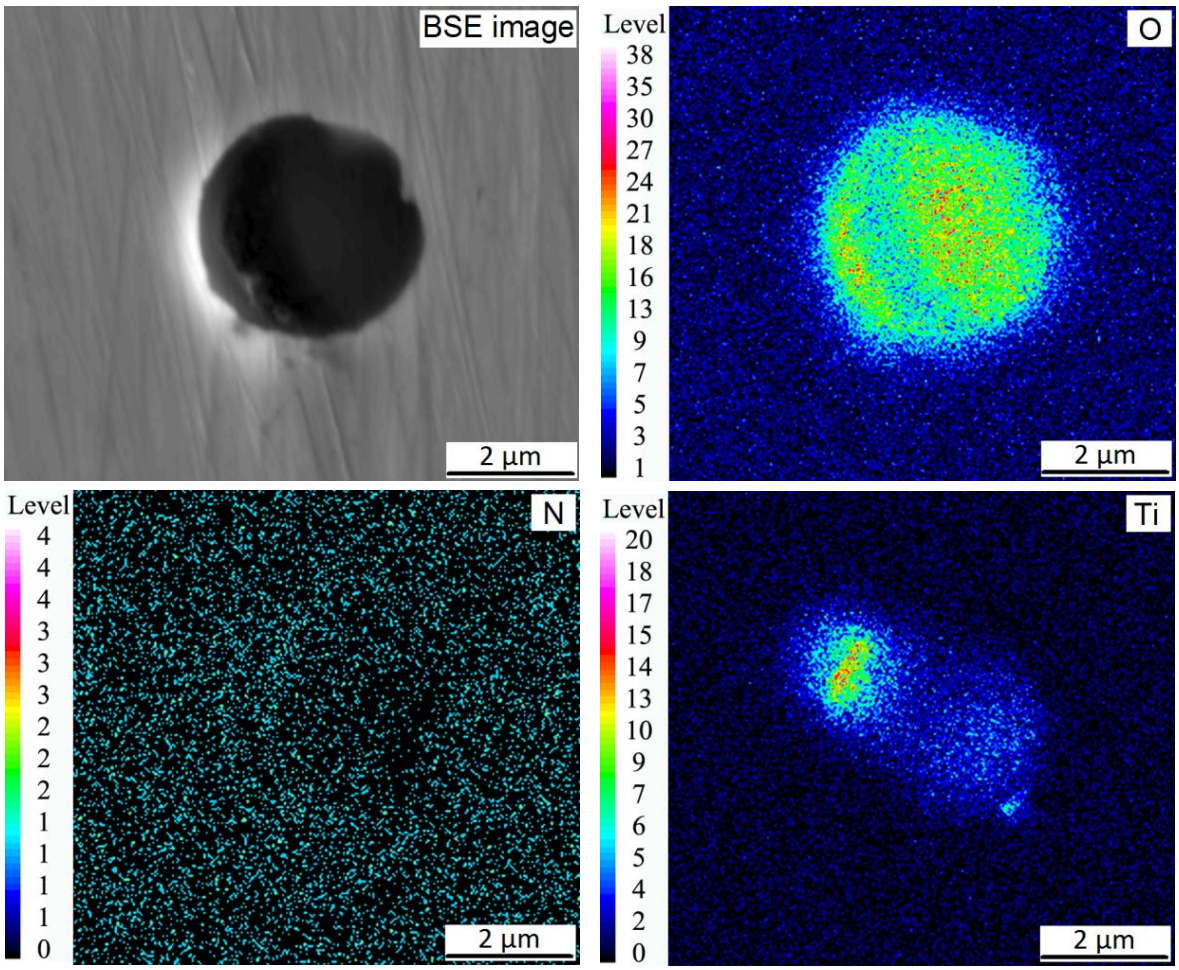

Fig. 5. Chemical composition characteristics of Ti-rich constituent in the inclusion in WH

constituents in respective solid solutions (i.e., titanial_spinel, ilmenite, pseudobrookite and corundum). It is worth noting that although titanial_spinel, ilmenite and pseudobrookite are all Ti-rich solid solutions, titanial_spinel and ilmenite have higher amounts of Mn, but lower Ti levels compared with pseudobrookite.

TABLE 3

Constituent contents of solid solutions (mass %)

Solid solutions	Constituents	Constituent contents of solid solutions in weld metals with different Al contents		
		0.01%	0.035%	0.085%
TiSp	$MnTi_2O_4$	77.9	—	—
	$MnAl_2O_4$	17.3	—	—
	$FeTi_2O_4$	1.92	—	—
IlME	$MnTiO_3$	92.1	53.5	—
	Ti_2O_3	7.83	43.1	—
	$FeTiO_3$	0.09	3.12	—
PSEU	Ti_3O_5	—	75.2	94.4
	$MnTi_2O_5$	—	22.5	5.34
	$FeTi_2O_5$	—	1.75	0.14
CORU	Al_2O_3	—	97.2	98.6
	Ti_2O_3	—	2.74	1.36

Note: "—" indicates the absence of solid solution under some Al contents of weld metals

TABLE 4

Chemical compositions of solid solutions (mass %)

Solid solutions	Elements	Compositions of solid solutions in weld metals with different Al contents		
		0.01%	0.035%	0.085%
TiSp	O	35.2	—	—
	Mn	32.6	—	—
	Ti	25.7	—	—
	Al	6.45	—	—
IlME	O	31.9	32.3	—
	Mn	33.5	27.5	—
	Ti	34.4	39.4	—
PSEU	O	—	35.5	36.5
	Mn	—	6.41	2.37
	Ti	—	57.3	59.5
CORU	O	—	46.3	46.7
	Al	—	50.3	51.5
	Ti	—	2.97	1.74

Note: Fe element is not listed in Table 4 because the contents in their respective solid solutions are very low (less than 1%)

Based on thermodynamic calculations shown in Figure 6, and Tables 3 and 4, it is clear that (Mn-Si-Al)-oxide appeared in EPMA analyses should be $Mn_2Al_4Si_5O_{18}$ compound, while Ti-containing phases are probably titanial_spinel, ilmenite

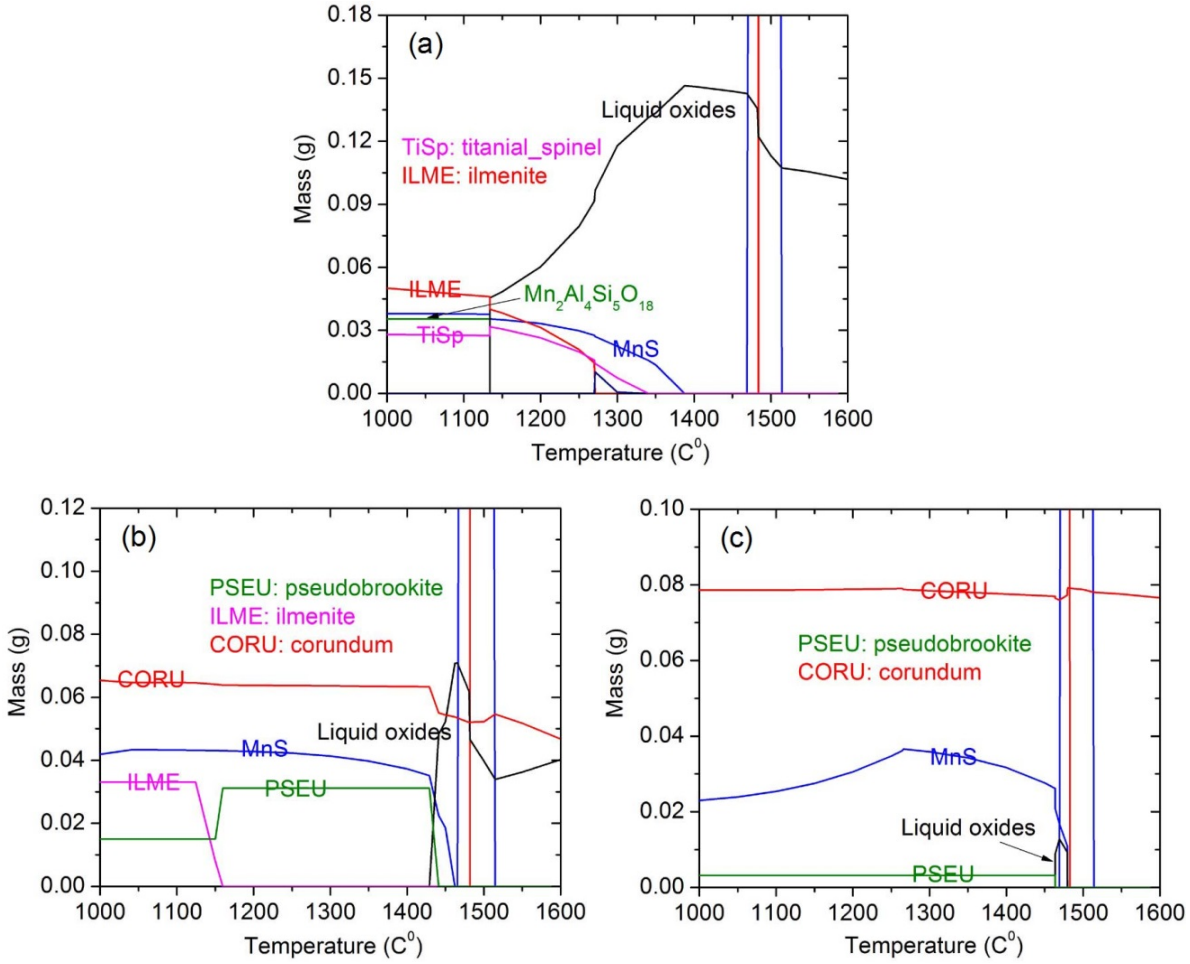

Fig. 6. The thermodynamic analyses on inclusions evolution for (a) WL, (b) WM and (c) WH. (The blue and red vertical lines represent the ferrite and austenite transformations, respectively)

and pseudobrookite. Additionally, Al-containing oxide phase in EPMA maps should be corundum and titanial_spinel. The phase identification analyses in Figures 7 and 8 further prove the conclusions described above. Comparisons between Figures 2-4 and the results of Figure 6 and Tables 3 and 4 show that thermodynamic analyses on constituents and chemical compositions characteristics of inclusions well agree with experimental results of EPMA maps.

Moreover, Figures 7 (a) and 8 (a) clearly show that several acicular ferrite (AF) plates emanate from the surface of an inclusion, indicating that the inclusion in WL has the ability to induce AF nucleation, while the inclusion in WH is inefficient for AF nucleation. Up to now, the formation of Mn-depleted zone (MDZ) is a generally accepted mechanism proposed for inducing the nucleation of AF on inclusions [2-5]. Accordingly, Mn concentration profile was measured by energy dispersive spectroscopy (EDS) spot analysis in the intervals of 10 nm within the range of 200 nm from the inclusion/matrix interface, and shown in Figure 9. It is clearly evident that a distinct drop in the Mn content can be detected around the inclusion containing substantial amounts of ilmenite and titanial_spinel solid solutions, whereas no variation in the Mn concentration is found in the matrix adjacent to the inclusion mainly composed of corundum.

As analyzed above, compared with pseudobrookite, ilmenite and titanial_spinel contain higher Mn content. Thus, in the case of the formation of a larger amounts of ilmenite and titanial_spinel in the inclusions, Mn in the surrounding matrix adjacent to the inclusion can be remarkably consumed, leading to a drop in the Mn content in the matrix in the vicinity of the inclusions. Meanwhile, due to the high cooling rate after welding, the Mn content around the inclusions can not be recovered to the equilibrium state by long-range diffusion of Mn located far from the inclusions [13]. Thus, the MDZ is formed in the matrix adjacent to the inclusions. In conclusion, the development of the MDZ is closely correlated with the presence of a large amount of Ti-containing and Mn-rich phases.

As mentioned above, Al element has a strong effect on the formation and evolution of inclusions in weld metals. It is well known that during welding, a series of complex metallurgical physics chemical reactions are expected to take place in weld pool. Elements Al, Ti, Si, Mn, etc., can combine with soluble oxygen in weld pool, which results in the formation of a variety of oxidation products such as Al_2O_3, TiO_x and MnO, and the decrease in the amount of the dissolved oxygen in the weld pool. There are the competition relationships between Al, Ti, Si and Mn during oxidation process. Compared with Si and Mn elements, Al

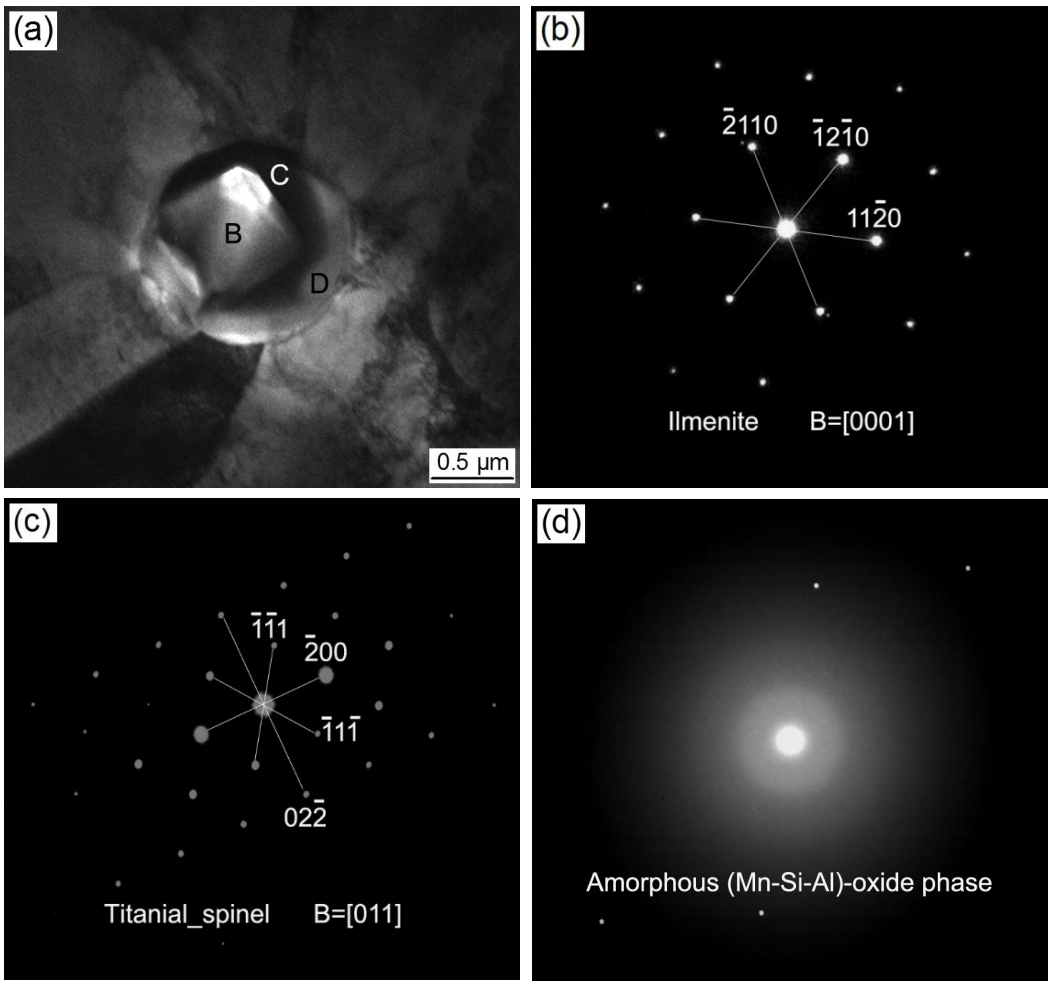

Fig. 7. SADP analyses for the main constituents of the inclusion in WL: (a) bright field image of inclusion, and (b)-(d) SADPs taken from regions B, C and D in (a), respectively

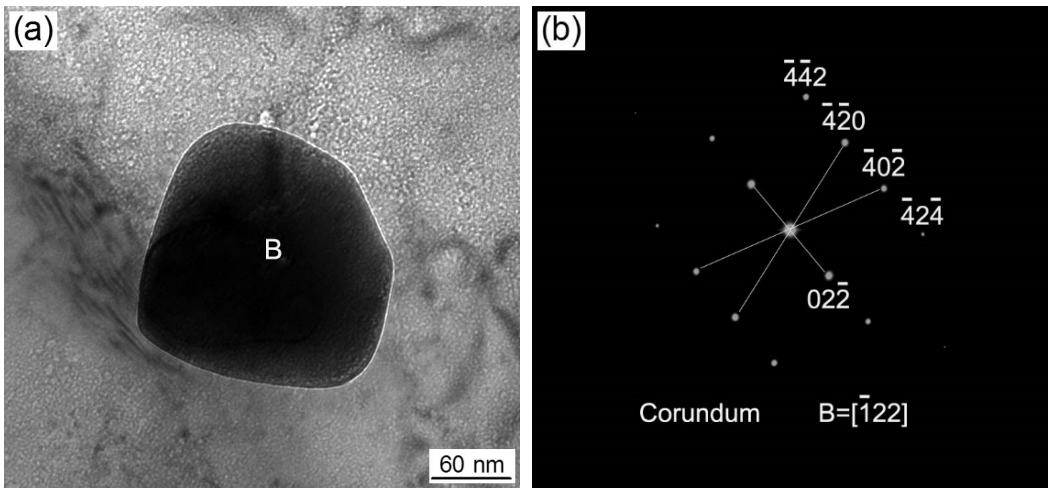

Fig. 8. SADP analyses for the main constituent of the inclusion in WH: (a) bright field image of inclusion, and (b) SADP taken from region B in (a)

and Ti have much stronger affinities with oxygen under the same contents due to their lower oxygen potentials of forming oxides (i.e., higher stability of oxide) [14]. Moreover, the content of metal elements also has a noticeable effect on the oxidation process of metals. In order to clarify the effect of Al content on the oxidation products, equilibrium calculation on compositions of oxidation products at 1600°C was carried out, and shown in Figure 10. Under low Al content (for example, 0.01% Al), despite high affinity with oxygen of Al, the amount of Al_2O_3 in oxidation products is lower compared with that of MnO due to high content of Mn

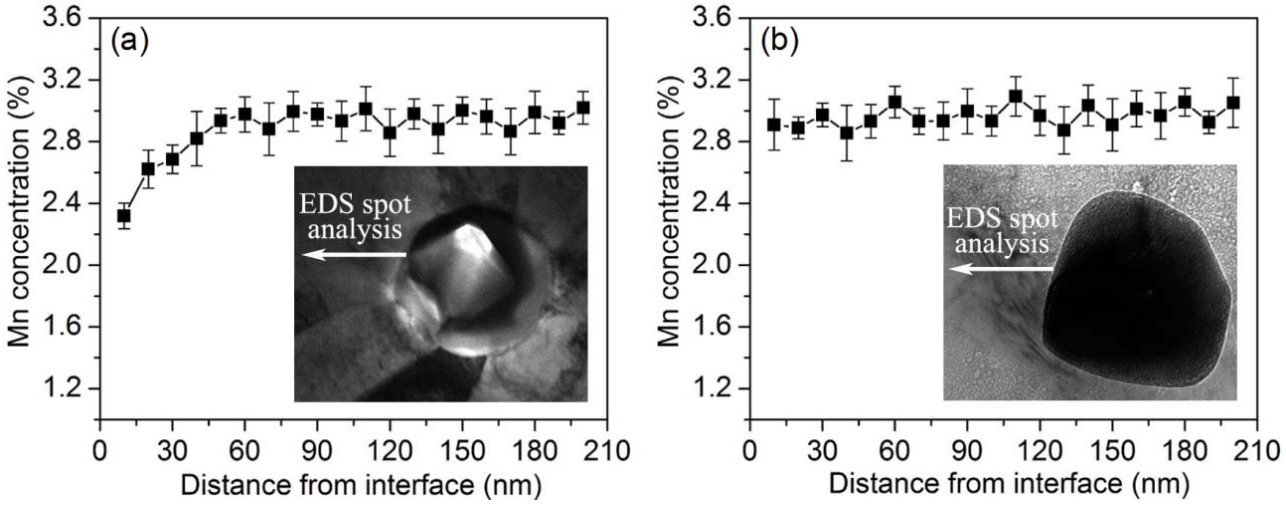

Fig. 9. Mn concentration profiles adjacent to the inclusions in (a) WL and (b)WH

element. With an increase in Al content, the amount of Al_2O_3 is strongly raised accompanied by the drops of other constituents. However, when content of Al is increased to the range of about 0.02-0.045%, the content of Al_2O_3 is slightly lowered, while those of Ti_2O_3 and TiO_2 are increased. The combining ability with oxygen for metals dissolved in Fe solution (i.e., oxygen potential of forming corresponding oxides) is determined as followed [14]:

$$\pi_{O(M_xO_y)} = \Delta_r G_m^{\ominus} + \frac{2}{y} RT \ln a_{(M_xO_y)} - \frac{2x}{y} RT \ln a_{[M]} \qquad (1)$$

Where $a_{(MxOy)}$ and $a_{[M]}$ denote the activities of M_xO_y in the liquid oxide and the metal element dissolved in liquid Fe solution, respectively, and $\Delta_r G_m^{\ominus}$ is the standard state oxygen potential of forming oxide. The liquid oxide and liquid Fe solutions can be regarded as ideal solutions. Thus, the concentrations of M_xO_y in the liquid oxide solution and the metal element dissolved in liquid Fe solution are respectively their activities [14].

When the Al content is increased up to a certain range (for example, 0.02-0.045%), the liquid oxides saturate in Al_2O_3 at the temperature higher than 1600°C, and solid state corundum is precipitated from the liquid oxide, as shown in Figure 6. At this time, $a_{(Al2O3)}$ reaches the maximum (namely one), which should increase the oxygen potential of forming Al_2O_3 according to Eq. [1], resulting in the decrease of the amount of Al_2O_3. Meanwhile, the amount of TiO_x can be increased due to the competition relationship between Al and Ti. When the content of Al is further increased (for example, more than 0.045%), according to Eq. [1], the oxygen potential of forming Al_2O_3 can be lowered due to the increases in $a_{[Al]}$ and constant $a_{(Al2O3)}$. Thus, a large amount of Al_2O_3 can precipitate in the form of solid state corundum, which strongly consumes soluble oxygen in liquid Fe solution. The decrease of soluble oxygen in liquid Fe solutions is expected to suppress the oxidation reactions of other metal elements including Ti [15,16], which leads to a remarkable decrease in the amounts of TiO_x, MnO, SiO_2 and so on, so that the amounts of MnO and SiO_2 are very low in the case of very high Al content, for example 0.085%.

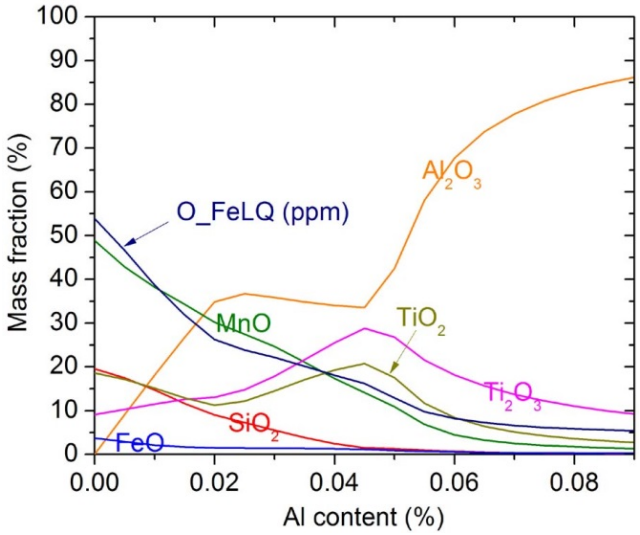

Fig. 10. The compositions of oxidation products at 1600°C calculated with Fe-0.05C-3.1Mn-0.23Si-0.014S-0.019Ti-0.039O-*x*Al ($0 < x < 0.09$) alloy system (in mass%) similar to the chemical compositions of weld metals . O_FeLQ (in ppm) represents dissolved oxygen content in liquid Fe solution at 1600°C

During cooling after welding, different kinds and amounts of constituent phases in inclusions are expected to precipitate in light of the chemical compositions characteristics of oxidation products. In the case of 0.01% Al, the oxidation product contains a large amount of MnO constituent and a certain amounts of TiO_x, which favours the formations of titanial_spinel and ilmenite rather than pseudobrookite. Similarily, the formation of (Mn-Si-Al)-oxide is also promoted due to high amount of MnO and a certain amount of SiO_2, as shown in Figure 2. When Al level is increased up to 0.035%, as analyzed above, the amounts of Ti_2O_3, TiO_2 and Al_2O_3 constituents in oxidation product are increased, but those of MnO and SiO_2 are correspondingly decreased, which results in an increase in the amounts of pseudobrookite and corundum at the expense of amounts of ilmenite and (Mn-Si-Al)-oxide in the inclusions, as shown in Figure 3. In the case of 0.085% Al,

the oxidation product is mainly composed of solid state Al_2O_3 with small amounts of TiO_x. Meanwhile, the amounts of SiO_2 and MnO in the oxidation product are very low, and in particular, the SiO_2 content is almost zero, resulting in the absence of (Mn-Si-Al)-oxide in the inclusions. Similarly, a very low content of MnO accompanied by small amounts of TiO_x contributes to the formation of a small amount of pseudobrookite. Thus, the inclusions have a very high amount of corundum and a very low content of pseudobrookite, as shown in Figure 4.

4. Conclusions

(1) The kinds and amounts of the constituent phases of the inclusions are remarkably changed with the Al content in the weld metals. The inclusions in the 0.01% Al weld metal are mainly composed of ilmenite with some amounts of (Mn-Si-Al)-oxide and titanial_spinel. When Al content is increased up to 0.035%, a more amount of corundum and a small amount of pseudobrookite are formed. In 0.085% Al weld metal, the (Mn-Si-Al)-oxide phase disappears completely, and the inclusions contain a substantial amount of corundum, in addition to a minimal amount of pseudobrookite.

(2) Ti_3O_5, $MnTi_2O_4$ and $MnTiO_3$ are the primary constituents of pseudobrookite, titanial_spinel and ilmenite solid solutions, respectively. Titanial_spinel and ilmenite have higher amounts of Mn, but lower Ti levels compared with pseudobrookite.

(3) In the case of presence of a considerable amounts of ilmenite and titanial_spinel, Mn-depleted zone is formed in matrix around the inclusions.

Acknowledgements

This work was financially supported by a Project of Education Department of Liaoning Province (grant no. L2016132).

REFERENCES

[1] A. Takada, Y.I. Komizo, H. Terasaki, T. Yokota, K. Oi, K. Yasuda, Welding Int. **29** (4), 254-261 (2015). doi: 10.1080/09507116.2014.921042.

[2] Y.B. Kang, H.G. Lee, ISIJ Int. **50** (4), 501-508 (2010). doi: 10.2355/isijinternational.50.501.

[3] Y.J. Kang, K.T. Han, J. H. Park, C.H. Lee, Metall. Mater. Trans. A **45**, 4753-4757 (2014). doi: 10.1007/s11661-014-2470-3.

[4] Y.J Kang, S.H. Jeong, J.H. Kang, C.H. Lee, Metall. Mater. Trans. A **47**, 2842-2854 (2016). doi: 10.1007/s11661-016-3456-0 .

[5] Y.J. Kang, J.H. Jang, J.H. Park, C.H. Lee, Met. Mater. Int. **20** (1), 119-127 (2014). doi: 10.1007/s12540-014-1013-1.

[6] X.D. Zou, J.C. Sun, D.P. Zhao, H. Matsuura, C. Wang, J. Iron Steel Res. Int. **25** (2), 164-172 (2018). doi: 10.1007/s42243-018-0022-6.

[7] X.D. Zou, D.P. Zhao, J.C. Sun, C. Wang, H. Matsuura, Metall. Mater. Trans. B **49** (2), 481-489 (2018). doi: 10.1007/s11663-017-1163-x.

[8] T.S. Zhang, C.J. Liu, M.F. Jiang, Metall. Mater. Trans. B **47**, 2253-2262 (2016). doi: 10.1007/s11663-016-0706-x.

[9] B.X. Wang, X.H. Liu, G.D Wang, Metall. Mater. Trans. A **49** (6), 2124-2138 (2018). doi:10.1007/s11661-018-4570-y.

[10] Q.S. Zhang, Y. Min, H.S. Xu, C.J. Liu, ISIJ Int. **58** (7), 1250-1256 (2018). doi: 10.2355/isijinternational.isijint-2018-105.

[11] J.Y. Li, G.G. Cheng, Q. Ruan, J.X. Pan, X.R. Chen, ISIJ Int. **58** (12), 2280-2287 (2018). doi: 10.2355/isijinternational.ISIJINT-2018-332.

[12] T.S. Zhang, C.J. Liu, J.Y. Qiu, X.B. Li, M.F. Jiang, ISIJ Int. **57** (2), 314-321 (2017). doi: 10.2355/isijinternational.ISIJINT2016-417.

[13] Y.J. Kang, K.T. Han, J.H. Park, C.H. Lee, Metall. Mater. Trans. A **46**, 3581-3591 (2015). doi: 10.1007/s11661-015-2958-5.

[14] H. Mitsutaka, I. Kimihisa, Thermodynamic data for steelmaking, Tohoku University Press, Japan, Sendai, 2010.

[15] Y.B Kang, S.H. Jung, ISIJ Int. **58** (8), 1371-1382 (2018). doi: 10.2355/isijinternational.ISIJINT-2018-198.

[16] K.C. Hsieh, S.S. Babu, J.M. Vitek, S.A. David, Mater. Sci. Eng. A **215**, 84-91 (1996). doi: 10.1016/0921-5093(96)10370-1.